DEVELOPMENT OF L-BAND PILLBOX RF WINDOW

Y.Takeuchi,S.Fukuda,H.Hisamatsu and Y.Saito
National Laboratory for High Energy Physics (KEK)
1-1 Oho,Tsukuba-shi,Ibaraki-ken,305,Japan

A.Takahashi
Mitsubishi Heavy Industries, Ltd. Mihara Machinery Works
5007 Itozaki-cho,Mihara-shi,Hiroshima-ken,729-03,Japan

Abstract

A pillbox RF output window was developed for the L-band pulsed klystron which will be used for the Japanese Hadron Project (JHP) 1-GeV proton linac. The window was designed to withstand a peak RF power of 6 MW, where the pulse width is 600 μsec and the repetition rate is 50 Hz. A high power test was successfully performed up to a 5.2 MW RF peak power with a 375 μsec pulse width and a 50 Hz repetition rate.

Introduction

Several R&D studies have been being carried out for the 1-GeV proton linac of JHP. Thirty-six L-band pulsed klystrons will be used in the high-β section of the JHP linac. The klystron will be required to have a 6 MW RF peak power, where the frequency is 1296 MHz, the pulse width is 600 μsec and a repetition rate is 50 Hz.[1] A prototype of the klystron is being developed at KEK. In a part of that work we have developed an L-band pillbox RF output window for the klystron. This window also can be used as an input RF window for the high-β coupled-cell cavity.

The pillbox type RF window is widely used as an output window of the high power klystron. Figure 1 shows a schematic drawing of a pillbox RF window. This type of window has the following advantages: 1) brazing of a ceramic disk to a copper sleeve is easier than that for rectangular structures; 2) an impedance matching is obtainable without an additional matching element such as an iris; 3) a pillbox window can be made to have a broad-band response by optimizing parameters. Therefore, we adopted the pillbox type window as the output window of the klystron.

The following procedures were carried out to develop the RF window. 1) An equivalent circuit model analysis on the impedance matching. 2) Optimization of the parameters by cold test. 3) Resonant mode study with "MAFIA" code and the cold test measurements. 4) Three dimensional field simulations with "MAFIA" and "HFSS" code.[2] 5) High power test. These procedures gave us much information to design an L-band pillbox window. Moreover, the results of our studies can be applied to the design of a window for other bands.

Criteria of design

Our design criteria for the pillbox window are as follows :1) the impedance matching of the window should be satisfied in a broad band ;2) to select a ceramic material which withstands a high electric field ;3) electric field near the ceramic is parallel to its surface and rather weak ;4) a thin film of TiN is coated on the surface of the ceramic to suppress multipactoring ;5) neither resonant modes in the pillbox nor ghost modes in the ceramic should be located near the operating frequency or its second harmonics ;6) the window structure is simple and can be fabricated easily at a low cost .

The first high-power model has been developed to satisfy all the criteria except the item 3).

Impedance matching on equivalent circuit

A pillbox window shown Fig.1 is considered as a transmission line which is composed of WR650 rectangular waveguides and a circular waveguide with a ceramic disk. Thus an equivalent circuit of the pillbox window is given as Fig. 2,[3] where B1 is a susceptance provided by step from rectangular to circular waveguide, Z1,Z2 and Z3 are the characteristic impedances of the WR650 rectangular waveguide, the circular waveguide and the circular waveguide filled with the ceramic material, respectively. It is assumed that only the TE_{10} mode can propagate in the rectangular waveguide and only the TE_{11} mode in the circular waveguide.

From the graphical analysis of this equivalent circuit on a Smith chart using typical parameters determined by measurements of a cold test model, we have obtained the following characteristics on the matching solutions.[4] 1) l_1 must be equal to l_2 when $l_1, l_2 < \lambda_g/2$,where λ_g is the guide wavelength. Here we define l_0 as $l_0 = l_1 = l_2$. 2) Two values of l_0 satisfy the impedance matching, when the thickness of the ceramic disk T is small enough and $l_0 < \lambda_g/2$. 3) There exists the maximum value of T which satisfies impedance matching, when $T < \lambda_g/2$. If T goes to the maximum value , two solutions of l_0 merge into one solution. When T is near the maximum value, the VSWR is not sensitive to the small deviation of l_0 from the solution. Therefore, this solution makes it possible to relax the tolerance for l. 4)Each of the solutions of l_1, l_2 and T has periodicity of $\lambda_g/2$. This means that if T is a solution , $T+N*\lambda_g/2$ is a solution too (where N=0,1,2,....). The periodicities of l_0 and T suggest feasibilities of a long type pillbox window and a pillbox window using a thick ceramic, respectively. The latter one is important to the design of a window for the higher frequencies such as the X band.

Cold test for optimizing parameters

The cold test models (diameter d=190 mm) were fabricated and studied precisely. Alumina ceramic disks HA997 and HA95 made by NTK co. are used. The ceramic thickness T was changed near the maximum value (where $T < \lambda_g/2$) described above from 5.0 mm to 7.4 mm.

Figure 3 shows frequency responses of VSWR obtained by the cold tests, where the ceramic is HA997 and T=5.0 mm. When l=40 mm, the VSWR curve has a bump between two dips. When l increases gradually, the right-hand dip moves toward the left-hand dip, the height of the bump decreases and the right-hand dip is merged with the left-hand dip (l=44 mm). The left-hand dip does not move when l increases from 38 mm to 44 mm. This means that the VSWR is not sensitive to a small change of l from the matching solution at the left-hand dip. This solution corresponds to the solution, discussed above, which has the maximum value of T. When T is increased gradually, both the dips move right hand. Thus we can adjust the frequency of the left-hand dip to the operating frequency by changing T. A broader bandwidth is available when the height of bump decreases before both the dips merge by changing l. This is shown as the solution of l=40 mm in Fig. 3. Figure 4 shows the frequency responses of the VSWR calculated with the equivalent circuit model. These curves are in good agreement with the data of the cold test. Several models are optimized using these data.

Resonant modes in pillbox RF window

A resonant mode in an RF window, whose frequency is located near the operating frequency, causes sometimes a serious failure. Therefore, the window design should be done to avoid resonances. We have studied resonant modes in a pillbox window by measurements of the cold test models, simulations using "MAFIA" code and calculations of ghost modes using the method proposed by Forrer and Jaynes.[5] Table 1 shows resonant modes in a pillbox RF window. The resonant modes are assigned by both the measurements and the simulations. The resonant frequencies obtained by the simulations using "MAFIA" are in good agreement with the ones by the measurements. But the frequencies of the ghost modes which are calculated assuming a long circular waveguide are different from the ones by the measurements, because field distributions of the resonant modes in the pillbox window near the operating frequency reach to steps from circular to rectangular waveguides. In this case, the resonant modes in the pillbox window are mainly dominated by its structure. In other words, the difference in cutoff frequencies between the cylinder part and the rectangular waveguide cause resonances. When the cutoff frequency of a certain mode in the

cylinder part is lower than that of the rectangular waveguide, a resonant mode is trapped in the cylinder part very often. This pillbox window has the TE_{111} modes, the TM_{010} mode and the TE_{211} modes shown in Table 1. The symmetric properties of the rectangular waveguide cause the frequency difference between the two polarizations. If a window is composed of a thick ceramic disk and a long cylinder, ghost modes appear clearly. Generally, a pillbox window is composed of a thin ceramic disk and a short cylinder i.e. $T<\lambda_g/2$ and $l_0<\lambda_g/2$. Thus the resonant modes in usual pillbox windows are seemed to be dominated by the structure of the pillbox.

Since the resonant frequency of the TM_{010} mode (1271MHz) is located near the operating frequency of 1296MHz, we are planing to increase the diameter of ceramic a little.

Field distribution in pillbox window

Three dimensional field calculations for the pillbox window have been done using "MAFIA" code and "HFSS" code. The mixing between the TM_{11} mode and the TE_{11} mode in a pillbox window was pointed out by Yamaguchi.[6] These modes exist also in the L-band window. Since the operating frequency is under the TM_{11} cutoff frequency of the circular waveguide, a long type pillbox window i.e. $l_0>\lambda_g/2$ can avoid the TM_{11} mode. However, we did not select a long type pillbox window, because of its size, weight and narrow-band response. From the experience of RF output windows for UHF klystrons used in TRISTAN, a lower slope of temperature rise (vs. RF power) by multipactoring was pointed out when a RF window has the parallel electric field distribution to the surface of the ceramic disk.[7),8)] Thus the long type pillbox window is expected to have good performance of smaller temperature rise by multipactoring.

Performance of high power test model

Two windows with the same dimensions (d=190 mm, T=5.8 mm and l=43 mm) were fabricated for the high power test. HA95 alumina ceramics were used for these windows. Both sides of the ceramic disk are coated with titanium nitride to suppress multipactoring. A 60 Å thick coating performed by ULCOAT co. is adopted, considering the fact that the optimized coating was found to be 60 to 150 Å thick performed by ULCOAT co. for the window ceramic of the UHF klystron used in TRISTAN.[7),8)]

Figure 5 shows the layout of the high power test. Each window is connected with an H-plane corner, inside of which is evacuated. The pressure was 10^{-9} Torr after a 72-hour baking at 100 °C. Three sapphire viewing ports are mounted to monitor glow emitted by discharge on the ceramic during the conditioning and to measure the ceramic temperature using an infrared thermometer. The RF power was fed by an L-band 5 MW klystron (THOMSON TH2104A).

During the conditioning, sudden gas bursts were observed frequently with or without emissions of blue-white glow. After 60-hour operation, the windows were conditioned up to the peak power level of 5.2 MW with a pulse width of 375 μsec and a repetition rate of 50 Hz, which was the maximum rating at that time limited by the RF source. Finally few gas bursts or few emissions of the glow were observed after the conditioning.

Figure 6 shows the dependence of the ceramic temperature on the transmitted power under the condition of a 375 μsec pulse width and a 50 Hz repetition rate. The open circles represent the measured temperatures. The solid curve is the fitting of measured data and extrapolated to 6 MW. Figure 7 shows the dependence of the ceramic temperature on the pulse width, where the peak RF power is 5.0 MW and the repetition rate is 50 Hz. The open circles represent the measured temperatures and the solid curve is the fitting of the measured data and extrapolated to 600 μsec. From Fig.6 and Fig. 7, the temperature of the ceramic becomes more than 220 °C when the peak power is 6 MW with a 600 μsec pulse width and a 50 Hz repetition rate. Since the thermal shock fracture resistance of the alumina ceramic decreases abruptly when the thermal shock exceeds 200 ~300 deg., the alumina ceramic should not be used over 200 °C. When we take into account the safety factor, the temperature rise of the ceramic should be less than 100 deg.. Therefore we should reduce the temperature rise of the ceramic disk.

The temperature rise of 78.5 deg. at 5 MW is higher than a value of 47.5 deg. roughly estimated from the dielectric loss of the ceramic material. More precise estimation of the temperature rise is necessary to evaluate the performance of the window. So we are planning to calculate the temperature rise and its distribution using a thermal analysis code and measure the dielectric loss including the effect of the TiN coating in the near future.

It is said that when the multipactoring occurs, the temperature rise is proportional to the 6~12th power of the RF power. However, the curve in Fig. 6 is almost linear to the peak RF power. Neither light emissions nor vacuum degradation was observed after conditioning. Thus the multipactoring was suppressed effectively by the TiN coating. Therefore the temperature rise of the ceramic is caused only by the dielectric loss and the ohmic loss. The loss tangents of HA95 and HA997 written in the catalog are 3×10^{-4} (at 1 MHz)and 3×10^{-5} (at 8 GHz) respectively. Thus, the next hot model is planed using HA997 and is expected better performance.

Conclusions

The pillbox RF window for the JHP L-band pulsed klystron was designed and studied precisely. Several models were optimized by the cold tests. One of these was tested and conditioned up to a 5.2 MW peak power with a 375 μsec pulse width and a 50 Hz repetition rate. The temperature rise due to the dielectric loss and the ohmic loss is too large to transmit a 6.0 MW peak RF power with a 600 μsec pulse width and a 50 Hz repetition rate. To improve this, the ceramic material HA997 with a smaller loss tangent will be used for the next hot model.

References

1)Report of the design study on the proton linac of the Japanese Hadron Project,No.1,JHP-10,KEK Internal 88-8,Sep. 1988.

2)"High-frequency structure simulator.",Catalog of Hewlett Packard Ltd. ,1990.

3)W.R.Fowkes , Stanford Linear Accelerator Center, Private communication.

4)Y.Takeuchi, "L-band output window", Report of the design study on the proton linac of the Japanese Hadron Project,No.2,JHP-14,KEK Internal 90-16,June 1990,pp. 259-277.

5) M.P.Forrer and E.T.Jaynes, "Resonant modes in waveguide windows", IRE Trans. on microwave theory tech.,vol.MTT-8, pp. 147-150, Mar. 1960.

6)S.Yamaguchi, Y.Saito and S.Anami, " Trajectory simulation of multipactoring electrons in a S-band pillbox RF window", Proceedings of the 15th linear accelerator meeting in Japan.,1990.

7)S.Isagawa, Y.Takeuchi, H.Baba, J.Tanaka, K.Ohya, Y.Kawakami and S.Hosoi, "Development of high power CW klystrons for TRISTAN", Proceedings of the IEEE particle accelerator conference, Washington, D.C., March,1987.

8)S.Isagawa and Y.Takeuchi, "Suppression of multipactoring on high power RF ceramic windows by TiN coating " , Proceedings of annual meeting of the surface finishing society of Japan, Nov. ,1991.

Table 1
Resonant Modes in Pillbox RF Window

Resonant frequency (Measured) MHz	Q value (Measured)	Resonant mode	Resonant frequency (Calculated) MHz
860	471	TE_{111}	894
1144	179	TE_{111}	1164
1271	417	TM_{010}	1263
1414	220	TE_{211}	1419
1425	199	TE_{211}	1428

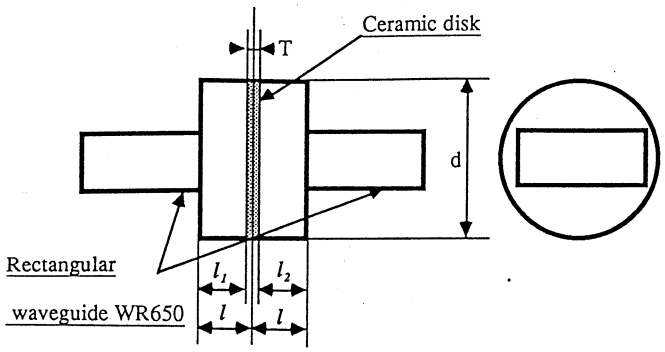

Fig.1 Structure of Pillbox RF Window

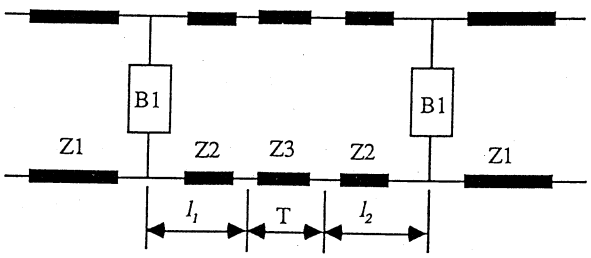

Fig.2 Equivalent Circuit of Pillbox RF Window

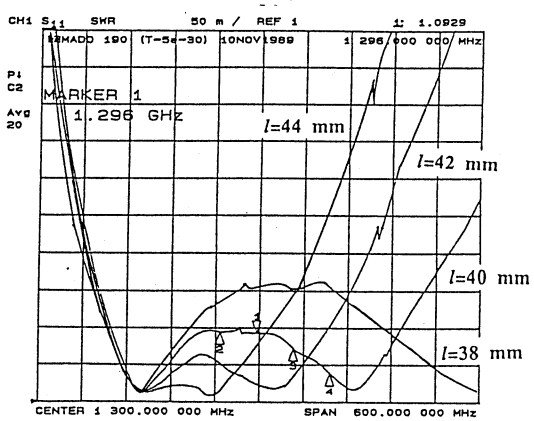

Fig.3 VSWR Curves of Cold Model, (Measured).
Horizontal axis range, 1000~1600 MHz.
Vertical axis range, 1.0~1.5.
(d=190 mm,T=5 mm,HA997,l=38~44 mm)

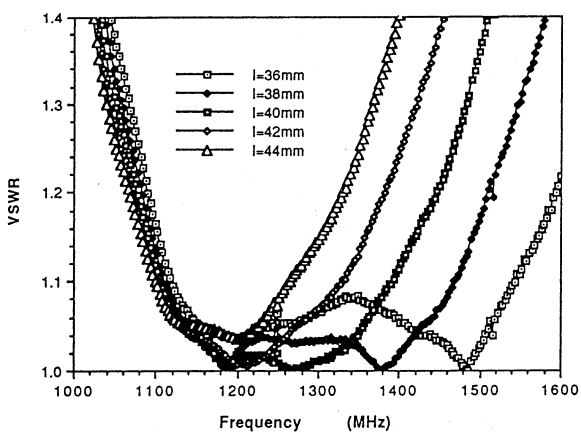

Fig.4 VSWR vs. Frequency, (calculated)

(d=190mm,T=5mm,HA997,l=36~44 mm)

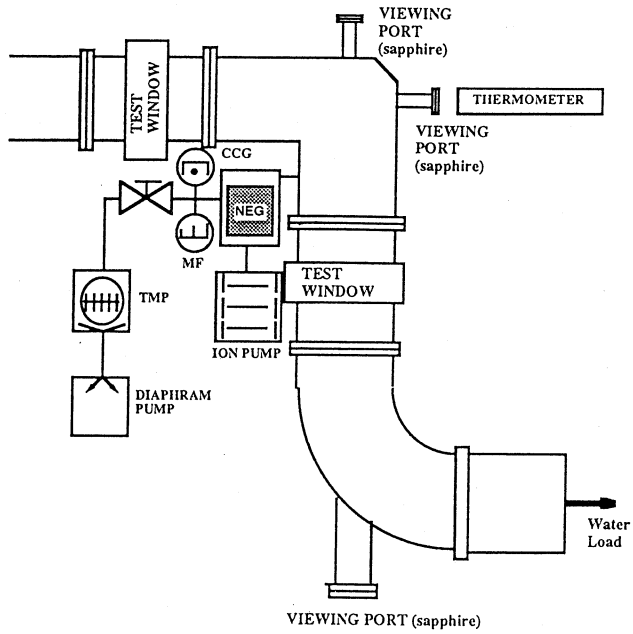

Fig. 5 Layout of High Power Test

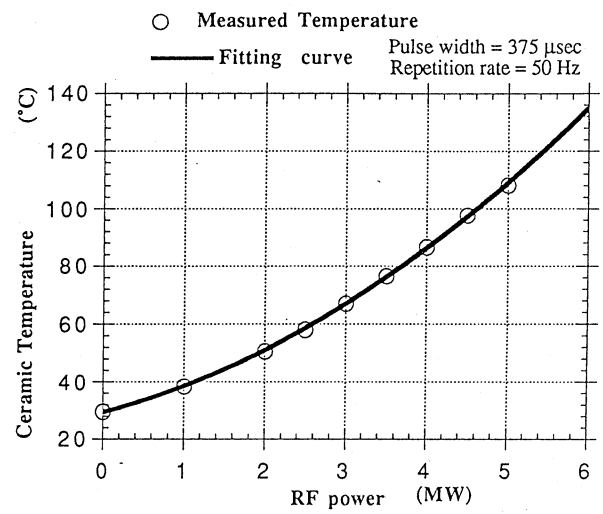

Fig. 6 Ceramic Temperature vs. RF Power

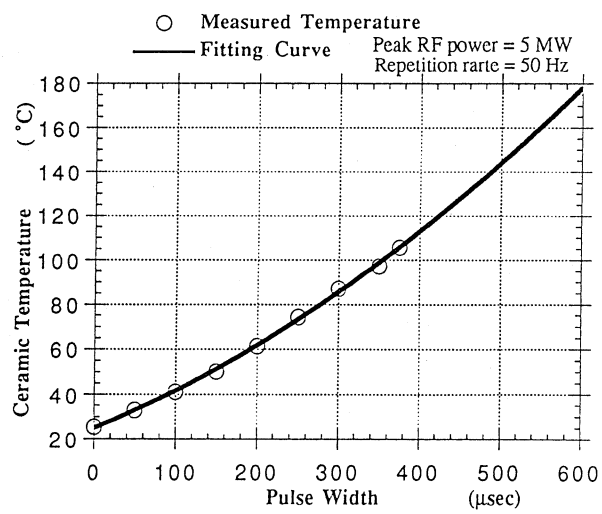

Fig.7 Ceramic Temperature vs. Pulse Width